NeuroImage: Clinical 23 (2019) 101815

Contents lists available at ScienceDirect

NeuroImage: Clinical

journal homepage: www.elsevier.com/locate/ynicl

Visual input drives increased occipital responsiveness and harmonized oscillations in multiple cortical areas in migraineurs

Jan Mehnert[a], Daniel Bader[a], Guido Nolte[b], Arne May[a,*]

[a] Department of Systems Neuroscience, University Medical Center Eppendorf, Hamburg, Germany
[b] Department of Neurophysiology and Pathophysiology, University Medical Center Eppendorf, Hamburg, Germany

ARTICLE INFO

Keywords:
Nociception
Trigeminal nervous system
Electroencephalography
Time-frequency analysis
Source localization
Functional coupling

ABSTRACT

Migraineurs are hypersensitive for most sensory domains like visual, auditory or somatosensory processing even outside of attacks. This behavioral peculiarity is mirrored by findings of cortical hyper-responsivity already in the interictal state. Using repetitive visual stimulation to elicit steady state visually evoked potentials (SSVEP) in 30 interictal episodic migraineurs and 30 controls we show hyper-responsivity of the visual cortex in the migraineurs. Additionally, the occipital regions were remarkably stronger coupled to the temporal, premotor and the anterior cingulate cortex than in headache free controls. These data suggest harmonized oscillations of different cortical areas as a response to visual input which might be driven by the cuneus. Furthermore, the increased coupling is modulated by the current state of the migraine cycle as the coupling was significantly stronger in patients with longer interictal periods.

1. Introduction

Hypersensitivity to sensory input is one of the core symptoms of the migraine attack (Schulte et al., 2015; Schulte and May, 2016) but in principle exists already interictally in migraineurs (Schwedt, 2013). This irritability to external input becomes pronounced in the preictal phase of the migraine cycle (Giffin et al., 2003; Laurell et al., 2016; Maniyar et al., 2015) which may explain the perception of prodromal symptoms. The migraine brain processes sensory input such as auditory (Ashkenazi et al., 2009; Vingen et al., 1998), olfactory (Demarquay et al., 2008; Stankewitz and May, 2011), somatosensory (Burstein et al., 2000), visual (Boulloche et al., 2010; Friedman and De ver Dye, 2009; Main et al., 2000) or nociceptive (Moulton et al., 2011) stimuli different than a non-migraine population, which has been discussed to be due to hyperresponsivity of primary sensory areas (Boulloche et al., 2010) or a lack of habituation in response to repetitive visual stimulation (Bjork et al., 2011; Coppola et al., 2013; de Tommaso et al., 2013; Magis et al., 2013).

Recently, it has been suggested that not only the individual primary sensory systems are altered but also multisensory processes (Boulloche et al., 2010; Noseda et al., 2010) raising the question whether multisensory integration (May, 2009; Schulte and May, 2017) and appraisal itself are also affected in migraine patients (Brighina et al., 2015; Schwedt, 2013).

To test our hypotheses of enhanced functional coupling in migraineurs during nociception and visual stimulation, we adapted a robust trigeminal pain model used in fMRI studies (Kröger and May, 2015; Schulte and May, 2016; Stankewitz et al., 2010) for electroencephalographic studies and compared interictal episodic migraineurs with healthy controls using concurrent source localization methods and measures of functional coupling.

2. Material and methods

2.1. Subjects and experimental design

Thirty-one female episodic interictal migraineurs (minimum of 24 h before and after the pervious/next attack) and 31 pairwise age matched female healthy volunteers without a history of headache participated. Male patients were not excluded, but since migraine is more common in females, by chance no male patient volunteered to take part in the study. The definition of migraine followed IHS classification (Headache Classification Committee of the International Headache Society (IHS), 2018) and all migraineurs filled out a migraine diary. Twelve migraineurs suffered from migraine with visual aura (fortifications). All patients reported increased sensitivity to light and nausea accompanying their attacks. 27 patients further report increased sensitivity to sound. All migraineurs were called after the day of the experiment until

* Corresponding author at: Department of Systems Neuroscience, University Medical Center Hamburg-Eppendorf, Martinistr. 52, 22046 Hamburg, Germany.
E-mail address: a.may@uke.de (A. May).

https://doi.org/10.1016/j.nicl.2019.101815
Received 31 January 2019; Received in revised form 29 March 2019; Accepted 2 April 2019
Available online 03 April 2019

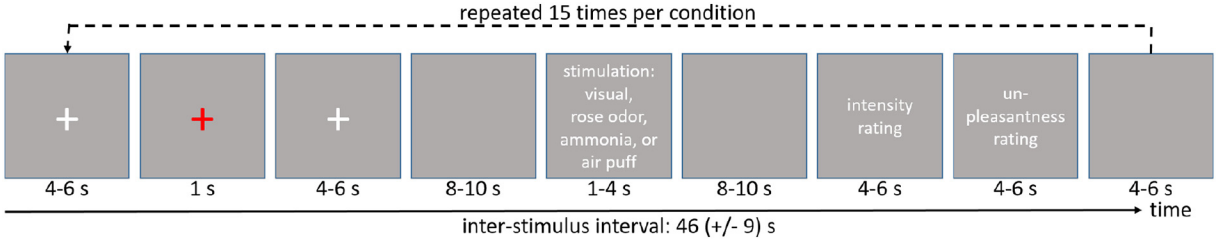

Fig. 1. Timeline of the experimental design. The red cross marks the onset of a reaction task to monitor the subjects attention. Actual stimuli are delivered either through a Teflon-tube with a constant stream of air into the subjects left nostril (for gaseous ammonia, rose odor, air puffs) or via a monitor (visual stimulation). After each trial the intensity and unpleasantness of the stimulus was rated. Each condition was repeated 15 times and trials were presented in randomized order.

the next attack occurred to define the number of days until next attack. The established paradigm (Mehnert et al., 2017; Schulte et al., 2016; Stankewitz et al., 2010) on nociception and visual excitation consists of separately applied 15 nociceptive, trigeminal stimuli (gaseous ammonia), 15 olfactory stimuli (gaseous rose odor) and 15 control stimuli (air puffs) to stimulate the trigeminal system. These three conditions were implemented as single boluses into a constant stream of air which flowed through a Teflon-tube into the participants left nostril. Additionally, all participants received 15 trials of binocular checkerboard stimulation. Stimuli were presented (jittered from 8 to 10 s) in a randomized order with the only constrain that two ammonia pulses where not allowed to follow each other directly to prevent habituation. After each stimulation, participants were asked to rate the intensity (in case of rose odor, air puffs and visual stimulation) or level of pain (in case of ammonia) on a scale from 0 to 100 (where 0 means no pain at all and 100 worst imaginable pain) and also unpleasantness on a scale from −50 to 50 (where −50 means very pleasant and 50 very unpleasant). The exact timing is shown in Fig. 1.

The repetitive visual stimulation used a circular flickering checkerboard pattern consisting of 5 rings each with 12 white or black squares. The patterns color (black/white) was reversed at a rate of 8 Hz to elicit steady state visually evoked potential (SSVEP) (Norcia et al., 2015). White was defined as highest and black as lowest possible luminance of the monitor. The stimuli were presented on a TFT Monitor (Samsung Syncmaster P2370(G), refreshing rate: 75 Hz, resolution: 1920 × 1080 pixel, length of diagonal: 23 in., width: 51 cm, height: 28.8 cm, reaction time of the monitor: 2 ms, max. luminance: 250 cd/m^2) controlled by a NVIDIA (Geforce GTX 1080) video card. The visual stimulus had a diameter of 14.8 cm and was in 75 cm distance from the subjects head. The horizontal and vertical visual angles are accordingly 10.9°. The background was throughout the experiment set to 50% gray (125 cd/m^2). Patients were seated vertically and horizontally centered relative to the screen's center.

During the experiment we measured electroencephalography (EEG) at 60 locations of the 10–20 system (Chatrian et al., 1985) at the head using a BrainAmp device (Brain Products, Germany) with active electrodes sampled at 1000 Hz. Four additional electrodes were used to obtain vertical and horizontal electrooculogram (EOG) to attenuate for eye movement and blinking artifacts. Two subjects (1 migraine, 1 control) were removed from the analysis due to artifacts. The final group therefore consisted of 30 migraineurs and 30 healthy controls for which we report the demographics in Table 1. Ethical approval was obtained from the local ethics authority (PV4896). Patients gave written informed consent.

2.2. Preprocessing of EEG data

EEG raw data were re-referenced to a common average, cut into epochs between −500 and 3000 ms regarding stimulus onset, and high-pass filtered at 0.5 Hz using the FieldTrip toolbox (Oostenveld et al., 2011). Powerline artifacts were reduced by a notch filter at 50 Hz. Eye movement and blinking artifacts were automatically eliminated by regressing out the electrode differences from the two vertical as well as from the two horizontal EOG channels using the procedure described by Parra and colleagues (Parra et al., 2005). Supplementary Fig. S1 demonstrates the (missing) correlation between EOG and EEG channels after artifact removal. Thereafter, all trials passed the automated muscle detection routine of FieldTrip and an overall z-score higher than 15. All identified artifact loaded trials were completely rejected from further analysis, leaving 94.9% of the trials (87.8% in ammonia condition, 95.9% in rose, 98.7% in checker and 97.3% in air condition) for the analysis. There were no significant differences in the number of remaining trials between groups over all trials as well as in the individual conditions (two-sample, two-tailed t-tests, all $p > .2$).

Time frequency transformation of the individual trials were calculated using the multi-taper method (Litvak et al., 2011; Mitra and Pesaran, 1999; Thomson, 1982) for frequencies window of 2 to 100 Hz with frequency step of 1 Hz and frequency resolution from 1 to 10 Hz, depending on the frequency under observation (higher resolution for higher frequencies) using the implementation of the SPM12 toolbox (http://www.fil.ion.ucl.ac.uk/spm/). Temporal resolution was set to 800 ms and the temporal steps to 50 ms. The resulting time-frequency spectra were - on a single trial level - recalculated as relative changes to baseline (defined as 500 to 0 ms before stimulus onset) by division, logarithmically transformed, and then averaged within the individuals showing the induced responses (David et al., 2006) following the robust averaging protocol within SPM12. Afterwards the individual averages were cropped to a temporal window from 0 to 2500 ms regarding stimulus onset.

Table 1
Demographic and clinical characteristics.

	Patients	Healthy Controls
N	30	30
Age (mean ± SD [min, max])	27,2 ± 6,6 (20, 45)	27.8 ± 8.0 (19,52)
Without Aura/with Aura	18/12	–
Days with headache per month (mean ± SD [min, max])	4,3 ± 2,7 (1, 12)	–
Attacks per Month	2,8 ± 2,1 (1, 8)	–
Duration of disease in years (≤11/12–17/≥ 18)	9/10/7	–
Days until next attack	16,29 ± 17,01 (2, 71)	–
Days after last attack	15,32 ± 11,33 (3, 55)	–

2.3. Analysis of time frequency dynamics

From the conditions “rose odor” and “ammonia” were subtracted the control condition “air puffs”. We then calculated a one sampled *t*-test for the main effect of nociception > control, rose > control and visual stimulation across all subjects and a further two sample t-test to show differences between healthy controls and migraineurs on smoothed (1 Hz, 500 ms Gaussian Kernel) image projections in the frequency range of 1 to 25 Hz at the electrodes Pz and Oz. These electrode positions were chosen from the literature regarding time-frequency responses after pain and trigeminal input (Grosser et al., 2000), or visual input, respectively. Results are reported positive if they passed the FWE-corrected threshold of $p < .05$. Frequency bands are defined as: beta 12.5–28 Hz, alpha 8–12 Hz, theta 3.5–7.5 Hz, and delta 0.5–3 Hz.

2.4. Source localization and phase coupling

We run source localization for the main effect of repetitive visual input with exact low resolution brain electromagnetic tomography (eLORETA) implemented into the MATLAB toolbox METH by Guido Nolte (https://www.uke.de/dateien/institute/neurophysiologie-und-pathophysiologie/downloads/meg_methods.zip) and using a lead-field with 5003 voxel covering the whole brain (cortex, midbrain and cerebellum) to locate power values from the cross-frequency-spectrum. We further used a linearly constrained minimum variance (LCMV) beamformer to show the consistency between both methods as suggested by Mahjoory et al. (2017). All voxel showing power change (dB) relative to baseline had to further pass FDR correction ($p < .05$) to deal with multiple comparison e.g. number of voxel. The peak voxel of the main effect of repetitive visual stimulation was used as a seed for the analysis on coupling differences by Multivariate Interaction Measure (MIM) in source space between migraineurs and healthy controls (Ewald et al., 2012). This method is a multivariate interaction measure, in fact a multivariate version of imaginary coherence, and is calculated here on source level to include all three source orientations for each voxel and does not require the specification of a source orientation. It is robust to artifacts of volume conduction and invariant to linear and static transformations of data within each voxel. Single subject results for each voxel entered a multivariate permutation test to assess group differences, since MIM-values are not normally distributed, and *p*-values were corrected with the *tmax*-method for multiple comparisons (Blair and Karniski, 1993; Groppe et al., 2011; Westfall and Young, 1993). This procedure was implemented in MATLAB by David Groppe (Version 1.1, https://de.mathworks.com/matlabcentral/fileexchange/54585-mult-comp-perm-t2). For visual inspection and to further test relations with clinical markers we also included results at an exploratory statistical threshold of $p < .01$ uncorrected.

2.5. Co-modulation with clinical markers of migraine

Behavioral data as well as results from the EEG (power in individual frequency bands, and coupling strength) were additionally tested for differences between patients with and without aura. Since we noticed quite long interictal periods in our patients with a broad variance (i.e. standard deviation), we also correlated the power of the individual frequency bands with the length of the interictal period as well as with the severity of the disease (Coppola et al., 2013). Results from the coupling analysis, i.e. the Multivariate Interaction Measure, were furthermore (non-parametrically) correlated with the patients' clinical parameters, (i) headache days per month, (ii) number of headache free days before, and (iii) after the EEG measurement by means of Spearman's rho.

2.6. Data availability

Unconditional access to anonymized data is available to qualified investigators on request to the corresponding author.

3. Results

3.1. Behavior

While two-sample, two-tailed *t*-tests did not reveal any significant differences in the intensity ratings between healthy controls and migraineurs, the unpleasantness ratings of the visual and rose odor were significantly ($p = .002$ and $p = .04$) higher in migraineurs compared to healthy controls. This effect was not seen in unpleasantness ratings of ammonia or air puff ratings (compare e.g. Mehnert and May, 2017). The behavior was not significantly different between patients with and without aura.

3.2. Time-frequency dynamics

The main effect of nociceptive stimulation showed significant increases in theta (for both electrodes of interest) and beta band (electrode Oz). Decreases could be shown in the alpha band after roughly 1.5 s regarding stimulus onset at electrode Pz. The comparison of migraineurs and healthy controls did not reveal significant differences in the nociceptive domain at the conservative threshold (FWE, $p < .05$) chosen. The main effect of visual stimulation was significant in three time-frequency clusters and showed a robust effect of SSVEP at 8 Hz in Oz (see Table 2 and Fig. 2). Contrasting migraineurs and healthy controls revealed increased power of the SSVEP (8 Hz) in a temporal

Table 2
Results for time-frequency analysis of the EEG, FWE corrected ($p < .05$) effects in the time-frequency domain.

Electrode position	Power increase (+) or decrease (−)	Frequency band	Frequency [Hz]	Time [ms]	T-value	p-Value (FWE-corrected)	Degree of freedom
Nociception							
Pz	+	Delta/theta	3–6	350–1150	5.58	0.000	59
	−	Alpha	9–10	1450–2000	3.75	0.014	59
Oz	+	Delta/theta	2–5	100–1800	7.97	0.000	59
	+	Beta	13–23	750–2000	4.40	0.003	59
Main effect visual							
Pz	+	Delta/theta/alpha	2–8	100–600	10.02	0.000	59
	−	Delta/theta	2–7	700–2000	10.37	0.000	59
	−	Beta	13–21	300–2000	8.95	0.000	59
Oz	+	Delta/theta/alpha	2–9	100–500	12.48	0.000	59
	+	Flickering (SSVEP)	8	100–2000	5.56	0.000	59
	−	Alpha	13	200–2000	6.20	0.000	59
	−	Delta/theta	2–6	700–2000	8.13	0.000	59
Group effect visual (controls < patients)							
Oz	+	Flickering (SSVEP)	8	350–1150	5.58	0.038	58

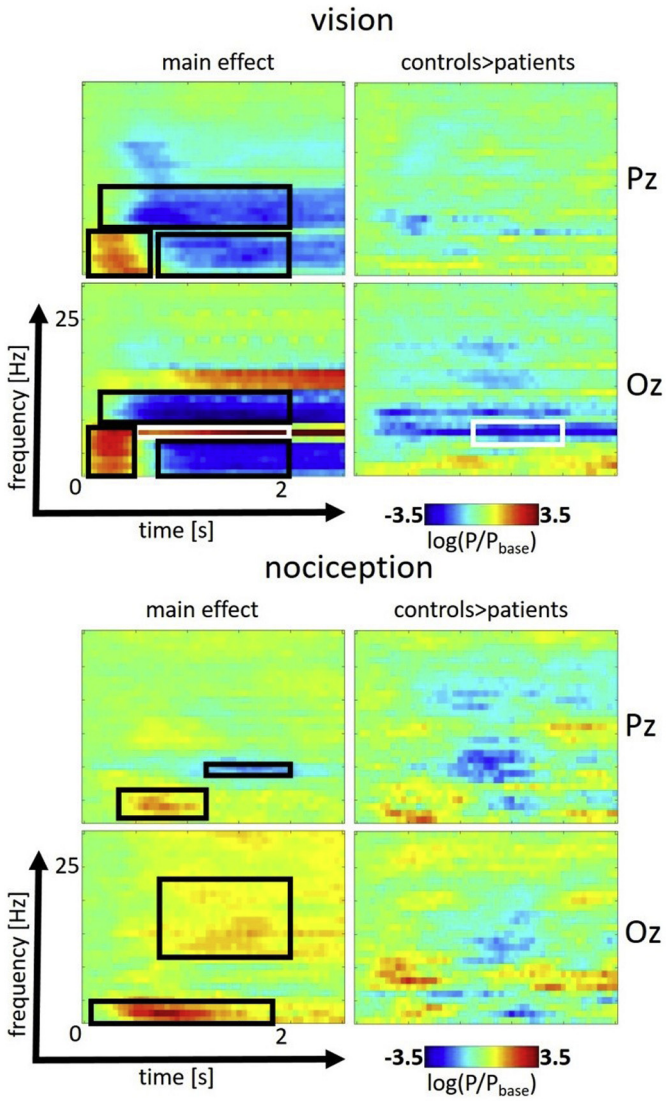

Fig. 2. Effect of visual repetitive (top) and trigeminal nociceptive stimulation (bottom) in the time-frequency domain from 0 to 2.5 s and 0 to 30 Hz for the electrodes Pz (top) and Oz (bottom). Significant effects (FWE-corrected, $p < .05$) are signified by black and - for the SSVEP - white rectangles. Displayed is the logarithmic transformation of power P relative to baseline power P_{base}.

window of 350 to 1150 ms regarding stimulus onset in patients only with an effect size of 1.46 (Cohen's d).

3.3. Source localization and coupling

The main effect of the SSVEP showed highest power in early visual areas (Cuneus, MNI coordinates 0, −83, 8 [xyz/mm]) (see Fig. 3, top) which was confirmed using the eLORETA and the LCVM beamformer as source localization tools (see Supplementary Fig. S2). The analysis of differences in coupling of the SSVEP showed that migraineurs had a significant (corrected for multiple comparison) increased coupling from early visual to two peak voxel located in the left temporal pole, more specifically at the coordinates [−68, −8 −23] and [−60, −8, −23] (xyz, mm in MNI-space, $p = .0404$ and $p = .0344$ adjusted for multiple comparisons, respectively). Visual inspection at lower statistical threshold (uncorrected, $p < .01$) further reveals increased coupling to two clusters namely left anterior cingulate cortex (ACC, peak voxel coordinate [−8, 38, 30]) and right premotor cortex (PMC) (peak voxel coordinate [30, 0, 68]) as shown in Fig. 3 (bottom).

3.4. Co-modulation with clinical markers of migraine

The MIM between Cuneus and the two aforementioned significant clusters in the middle temporal gyrus (MTG) ($r = 0.340$, $p = .035$ and $r = 0.370$, $p = .024$, respectively) and the ACC ($r = 0.467$, $p = .005$) correlated positively with the number of headache free days before the experiment (Spearman's Rho, one sided test) see Fig. 4. This means that the coupling was stronger the longer the duration of the last attack. No correlation (positive or negative) was found regarding the coupling of the cuneus and any cortical areas with the days until the next attack. We found no significant differences between patients with and without aura. Furthermore the severity and length of the interictal period was not correlated to the power of the individual frequency bands in neither of the two conditions.

4. Discussion

Although our nociceptive stimulation paradigm showed robust results in fMRI (Schulte et al., 2017; Schulte and May, 2016; Stankewitz and May, 2011) and reproduced pain related electrophysiological effects such as increases in theta- and decreases in alpha band (Huart et al., 2012; Ploner et al., 2006; Taesler and Rose, 2016) we did not find significant differences in nociceptive processing between migraineurs and controls despite investigating rather large groups. Such differences are therefore mainly either sub-cortical (brainstem (Weiller et al., 1995), thalamus (Noseda et al., 2011), hypothalamus (Schulte and May, 2016)) and therefore not accessible by EEG, or rather subtle alterations in the cortical transmission of nociceptive input in migraineurs. Another possibility is that such differences exist but perhaps more in the ictal phase. Although there are some reports about visual stimulation and EEG changes in migraine patients (Bjork et al., 2011; Coppola et al., 2013; de Tommaso et al., 2013), we note a surprising lack of such data regarding trigeminal pain and nociceptive input (de Tommaso et al., 2015).

In contrast to the nociceptive system, the neuronal response following visual input showed robust differences between groups: Interictally, episodic migraineurs showed a significant higher activation of the primary visual area (cuneus) in response to repetitive visual stimulation. This increased response was notably in the same frequency band as the visual input flicker, corresponding to steady-state visually evoked potentials (SSVEP). This finding can be seen in the light of a lack of habituation to slowly flickering light in migraineurs. Of note, fast flickering frequencies around 20 Hz, known as photic driving, show inconsistent results (Chorlton and Kane, 2000; Fogang et al., 2015). Nevertheless, similar findings of a lack of habituation are known to happen in migraine patients also in other sensory domains (Magis et al., 2016, 2013) and have been discussed as a hyperresponsive cortical reaction to sensory (here: visual) input. Hyperresponsivity to visual stimulation in interictal migraine patients has also been reported in a previous PET study (Boulloche et al., 2010) for two different light intensities, and also in fMRI (Huang et al., 2011). More importantly, using concurrent analyzing methods of inter-regional coupling invariant to volume conduction we could link this finding to other cortical hubs, especially the temporal pole (Cortese et al., 2017; Moulton et al., 2011), the premotor cortex and the ACC. Although altered functional connectivities have been reported in healthy subjects following stressful visual stimulation (Huang and Zhu, 2017), our finding of enhanced functional connectivity of the aforementioned cortical areas is remarkable as it shows harmonized oscillations of widespread cortical areas as a response to visual input. This finding prompts the question whether the hypersensitive appearance of migraineurs, known to have lower detection thresholds in numerous sensory dimensions (pain, heat, vision, auditory, touch (Hodkinson et al., 2015)) and altered thresholds in contrast detection and orientation (O'Hare and Hibbard, 2016; Tibber et al., 2006), may indeed prove to be due to a generally altered stimulus-response pattern of the migraine brain. This migraine specific

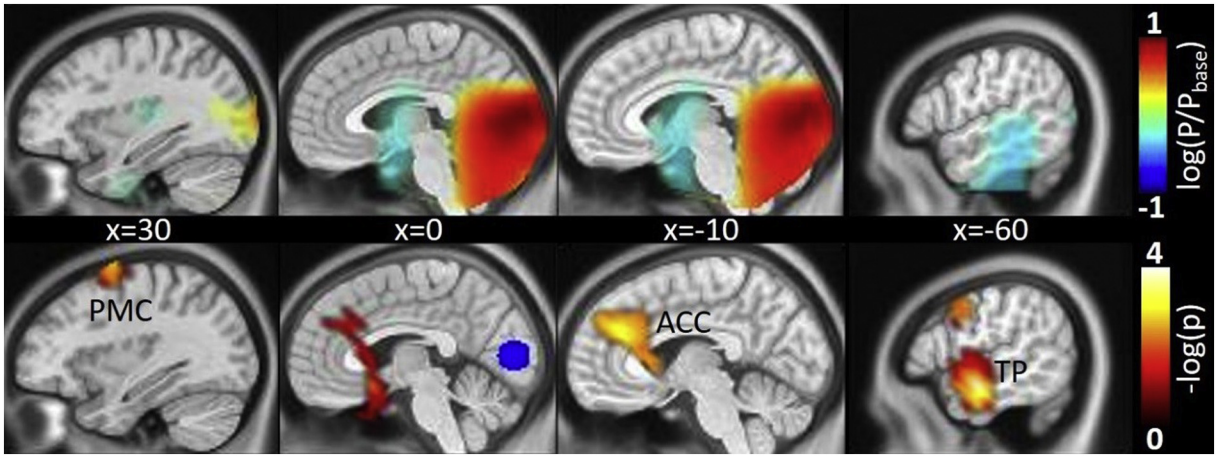

Fig. 3. Source localization of the FDR-corrected ($p < .05$) main effect (in logarithmic transformation of power P relative to baseline power P_{base}) of repetitive visual stimulation (top) and increased coupling in the migraineurs (bottom) to premotor cortex (PMC), anterior cingulate cortex (ACC) and temporal pole (TP) by means of multivariate interaction measure (MIM) taking the peak voxel of the main effect as seed (marked in blue) for the phase (noted as negative decadic logarithmic transformation of uncorrected p-values lower than 0.01). Sagittal slices are presented for 4 x-coordinates in MNI space.

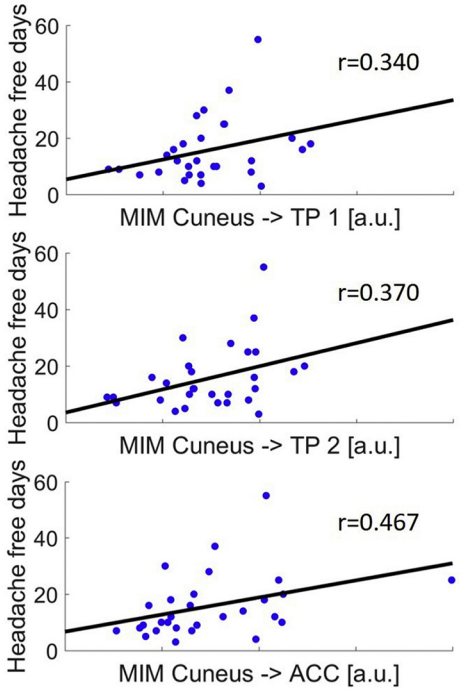

Fig. 4. Significant correlation (Spearman) of headache free days since the last migraine attack and coupling strength from cuneus to both locations in the temporal pole (TP 1 and TP 2) and anterior cingulate cortex (ACC).

stimulus-response pattern would meet and possibly drive oscillations in specific single brain areas such as the thalamus or hypothalamus which are currently thought to define thresholds and generate impulses for attack generation (Akerman et al., 2011; Bahra et al., 2001; Mehnert and May, 2017; Schulte and May, 2016; Stankewitz and May, 2011).

Our data show not only generally elevated levels of coupling between the visual system, the motor system, the temporal pole and ACC but link them to the cycling of the disease, as the activity correlation within these systems and the days since the last attack increases.

Perception changes of sensory input during a migraine cycle are a continuum across different phases with a different magnitude of sensitivity (Laurell et al., 2016; Maniyar et al., 2015; Schulte et al., 2015), but also a different connectivity strength of cortical coupling. This is further evidence for a migraine specific disturbance in cortical processing and underlines the importance to focus on migraine cyclic behavior when investigating this disease. We note that we could not show a correlation towards the next attack which may be due to the higher variance of days towards the next attack in our cohort. It may be necessary to investigate patients with a higher attack frequency to prove such correlations. Nevertheless, our finding suggest migraine specific alterations of cortical pathways which is in line with recent results gained from resting-state fMRI (Hodkinson et al., 2017).

Acknowledgement

This work was supported by the German Research Foundation, SFB936/A5 to A.M., and SFB936/Z3 to G.N.

Appendix A. Supplementary data

Supplementary data to this article can be found online at https://doi.org/10.1016/j.nicl.2019.101815.

References

Akerman, S., Holland, P.R., Goadsby, P.J., 2011. Diencephalic and brainstem mechanisms in migraine. Nat. Rev. Neurosci. 12, 570–584. https://doi.org/10.1038/nrn3057.

Ashkenazi, A., Mushtaq, A., Yang, I., Oshinsky, M.L., 2009. Ictal and interictal phonophobia in migraine-a quantitative controlled study. Cephalalgia 29, 1042–1048. https://doi.org/10.1111/j.1468-2982.2008.01834.x.

Bahra, A., Matharu, M.S., Büchel, C., Frackowiak, R.S., Goadsby, P.J., 2001. Brainstem activation specific to migraine headache. Lancet 357, 1016–1017.

Bjork, M., Hagen, K., Stovner, L., Sand, T., 2011. Photic EEG-driving responses related to ictal phases and trigger sensitivity in migraine: a longitudinal, controlled study. Cephalalgia 31, 444–455. https://doi.org/10.1177/0333102410385582.

Blair, R.C., Karniski, W., 1993. An alternative method for significance testing of waveform difference potentials. Psychophysiology 30, 518–524.

Boulloche, N., Denuelle, M., Payoux, P., Fabre, N., Trotter, Y., Géraud, G., 2010. Photophobia in migraine: an interictal PET study of cortical hyperexcitability and its modulation by pain. J. Neurol. Neurosurg. Psychiatry 81, 978–984. https://doi.org/10.1136/jnnp.2009.190223.

Brighina, F., Bolognini, N., Cosentino, G., Maccora, S., Paladino, P., Baschi, R., Vallar, G., Fierro, B., 2015. Visual cortex hyperexcitability in migraine in response to sound-induced flash illusions. Neurology 84, 2057–2061. https://doi.org/10.1212/WNL.0000000000001584.

Burstein, R., Yarnitsky, D., Goor-Aryeh, I., Ransil, B.J., Bajwa, Z.H., 2000. An association between migraine and cutaneous allodynia. Ann. Neurol. 47, 614–624.

Chatrian, G.E., Lettich, E., Nelson, P.L., 1985. Ten Percent electrode system for topographic studies of spontaneous and evoked EEG activities. Am. J. EEG Technol. 25, 83–92. https://doi.org/10.1080/00029238.1985.11080163.

Chorlton, P., Kane, N., 2000. Investigation of the cerebral response to flicker stimulation in patients with headache. Clin. Electroencephalogr. 31, 83–87.

Coppola, G., Parisi, V., Di Lorenzo, C., Serrao, M., Magis, D., Schoenen, J., Pierelli, F., 2013. Lateral inhibition in visual cortex of migraine patients between attacks. J. Headache Pain 14, 20. https://doi.org/10.1186/1129-2377-14-20.

Cortese, F., Pierelli, F., Bove, I., Di Lorenzo, C., Evangelista, M., Perrotta, A., Serrao, M., Parisi, V., Coppola, G., 2017. Anodal transcranial direct current stimulation over the left temporal pole restores normal visual evoked potential habituation in interictal migraineurs. J. Headache Pain 18, 70. https://doi.org/10.1186/s10194-017-0778-2.

David, O., Kilner, J.M., Friston, K.J., 2006. Mechanisms of evoked and induced responses in MEG/EEG. NeuroImage 31, 1580–1591. https://doi.org/10.1016/j.neuroimage.2006.02.034.

de Tommaso, M., Stramaglia, S., Marinazzo, D., Trotta, G., Pellicoro, M., 2013. Functional and effective connectivity in EEG alpha and beta bands during intermittent flash stimulation in migraine with and without aura. Cephalalgia 33, 938–947. https://doi.org/10.1177/0333102413477741.

de Tommaso, M., Trotta, G., Vecchio, E., Ricci, K., Van de Steen, F., Montemurno, A., Lorenzo, M., Marinazzo, D., Bellotti, R., Stramaglia, S., 2015. Functional connectivity of EEG signals under laser stimulation in migraine. Front. Hum. Neurosci. 9. https://doi.org/10.3389/fnhum.2015.00640.

Demarquay, G., Royet, J.P., Mick, G., Ryvlin, P., 2008. Olfactory hypersensitivity in migraineurs: a H(2)(15)O-PET study. Cephalalgia 28, 1069–1080. https://doi.org/10.1111/j.1468-2982.2008.01672.x.

Ewald, A., Marzetti, L., Zappasodi, F., Meinecke, F.C., Nolte, G., 2012. Estimating true brain connectivity from EEG/MEG data invariant to linear and static transformations in sensor space. Neuroimage 60, 476–488. https://doi.org/10.1016/j.neuroimage.2011.11.084.

Fogang, Y., Gerard, P., De Pasqua, V., Pepin, J.L., Ndiaye, M., Magis, D., Schoenen, J., 2015. Analysis and clinical correlates of 20 Hz photic driving on routine EEG in migraine. Acta Neurol. Belg. 115, 39–45. https://doi.org/10.1007/s13760-014-0309-8.

Friedman, D.I., De ver Dye, T., 2009. Migraine and the environment. Headache 49, 941–952. https://doi.org/10.1111/j.1526-4610.2009.01443.x.

Giffin, N.J., Ruggiero, L., Lipton, R.B., Silberstein, S.D., Tvedskov, J.F., Olesen, J., Altman, J., Goadsby, P.J., Macrae, A., 2003. Premonitory symptoms in migraine: an electronic diary study. Neurology 60, 935–940.

Groppe, D.M., Urbach, T.P., Kutas, M., 2011. Mass univariate analysis of event-related brain potentials/fields II: simulation studies. Psychophysiology 48, 1726–1737. https://doi.org/10.1111/j.1469-8986.2011.01272.x.

Grosser, K., Oelkers, R., Hummel, T., Geisslinger, G., Brune, K., Kobal, G., Lötsch, J., 2000. Olfactory and trigeminal event-related potentials in migraine. Cephalalgia 20, 621–631.

Headache Classification Committee of the International Headache Society (IHS), 2018. The international classification of headache disorders, 3rd edition. Cephalalgia 38, 1–211.

Hodkinson, D.J., Veggeberg, R., Wilcox, S.L., Scrivani, S., Burstein, R., Becerra, L., Borsook, D., 2015. Primary somatosensory cortices contain altered patterns of regional cerebral blood flow in the interictal phase of migraine. PLoS One 10, e0137971. https://doi.org/10.1371/journal.pone.0137971.

Hodkinson, D.J., Veggeberg, R., Kucyi, A., van Dijk, K.R.A., Wilcox, S.L., Scrivani, S.J., Burstein, R., Becerra, L., Borsook, D., 2017. Cortico–cortical connections of primary sensory areas and associated symptoms in migraine. eNeuro 3. https://doi.org/10.1523/ENEURO.0163-16.2016.

Huang, J., Zhu, D.C., 2017. Visually stressful striped patterns alter human visual cortical functional connectivity. Hum. Brain Mapp. 38, 5474–5484. https://doi.org/10.1002/hbm.23740.

Huang, J., Zong, X., Wilkins, A., Jenkins, B., Bozoki, A., Cao, Y., 2011. fMRI evidence that precision ophthalmic tints reduce cortical hyperactivation in migraine. Cephalalgia 31, 925–936. https://doi.org/10.1177/0333102411409076.

Huart, C., Legrain, V., Hummel, T., Rombaux, P., Mouraux, A., 2012. Time-frequency analysis of chemosensory event-related potentials to characterize the cortical representation of odors in humans. PLoS One 7, e33221. https://doi.org/10.1371/journal.pone.0033221.

Kröger, I.L., May, A., 2015. Triptan-induced disruption of trigemino-cortical connectivity. Neurology 84, 2124–2131. https://doi.org/10.1212/WNL.0000000000001610.

Laurell, K., Artto, V., Bendtsen, L., Hagen, K., Häggström, J., Linde, M., Söderström, L., Tronvik, E., Wessman, M., Zwart, J.A., Kallela, M., 2016. Premonitory symptoms in migraine: a cross-sectional study in 2714 persons. Cephalalgia 36, 951–959. https://doi.org/10.1177/0333102415620251.

Litvak, V., Mattout, J., Kiebel, S., Phillips, C., Henson, R., Kilner, J., Barnes, G., Oostenveld, R., Daunizeau, J., Flandin, G., Penny, W., Friston, K., 2011. EEG and MEG data analysis in SPM8. Comput. Intel. Neurosci. 2011, e852961. https://doi.org/10.1155/2011/852961.

Magis, D., Vigano, A., Sava, S., d'Elia, T.S., Schoenen, J., Coppola, G., 2013. Pearls and pitfalls: electrophysiology for primary headaches. Cephalalgia 33, 526–539. https://doi.org/10.1177/0333102413477739.

Magis, D., Lisicki, M., Coppola, G., 2016. Highlights in migraine electrophysiology: are controversies just reflecting disease heterogeneity? Curr. Opin. Neurol. 29, 320–330. https://doi.org/10.1097/WCO.0000000000000335.

Mahjoory, K., Nikulin, V.V., Botrel, L., Linkenkaer-Hansen, K., Fato, M.M., Haufe, S., 2017. Consistency of EEG source localization and connectivity estimates. Neuroimage 152, 590–601. https://doi.org/10.1016/j.neuroimage.2017.02.076.

Main, A., Vlachonikolis, I., Dowson, A., 2000. The wavelength of light causing photophobia in migraine and tension-type headache between attacks. Headache 40, 194–199.

Maniyar, F.H., Sprenger, T., Monteith, T., Schankin, C.J., Goadsby, P.J., 2015. The premonitory phase of migraine–what can we learn from it? Headache 55, 609–620. https://doi.org/10.1111/head.12572.

May, A., 2009. New insights into headache: an update on functional and structural imaging findings. Nat. Rev. Neurol. 5, 199–209.

Mehnert, J., May, A., 2017. Functional and structural alterations in the migraine cerebellum. J. Cereb. Blood Flow Metab. https://doi.org/10.1177/0271678X17722109. 271678X17722109.

Mehnert, J., Schulte, L., Timmann, D., May, A., 2017. Activity and connectivity of the cerebellum in trigeminal nociception. Neuroimage 150, 112–118. https://doi.org/10.1016/j.neuroimage.2017.02.023.

Mitra, P.P., Pesaran, B., 1999. Analysis of dynamic brain imaging data. Biophys. J. 76, 691–708. https://doi.org/10.1016/S0006-3495(99)77236-X.

Moulton, E.A., Becerra, L., Maleki, N., Pendse, G., Tully, S., Hargreaves, R., Burstein, R., Borsook, D., 2011. Painful heat reveals hyperexcitability of the temporal pole in interictal and ictal migraine States. Cereb. Cortex 21, 435–448. https://doi.org/10.1093/cercor/bhq109.

Norcia, A.M., Appelbaum, L.G., Ales, J.M., Cottereau, B.R., Rossion, B., 2015. The steady-state visual evoked potential in vision research: a review. J. Vis. 15, 4. https://doi.org/10.1167/15.6.4.

Noseda, R., Kainz, V., Jakubowski, M., Gooley, J.J., Saper, C.B., Digre, K., Burstein, R., 2010. A neural mechanism for exacerbation of headache by light. Nat. Neurosci. 13, 239–245. https://doi.org/10.1038/nn.2475.

Noseda, R., Jakubowski, M., Kainz, V., Borsook, D., Burstein, R., 2011. Cortical projections of functionally identified thalamic trigeminovascular neurons: implications for migraine headache and its associated symptoms. J. Neurosci. 31, 14204–14217. https://doi.org/10.1523/JNEUROSCI.3285-11.2011.

O'Hare, L., Hibbard, P.B., 2016. Visual processing in migraine. Cephalalgia 36, 1057–1076. https://doi.org/10.1177/0333102415618952.

Oostenveld, R., Fries, P., Maris, E., Schoffelen, J.-M., 2011. FieldTrip: Open Source Software for Advanced Analysis of MEG, EEG, and Invasive Electrophysiological Data [WWW Document]. https://doi.org/10.1155/2011/156869.

Parra, L.C., Spence, C.D., Gerson, A.D., Sajda, P., 2005. Recipes for the linear analysis of EEG. Neuroimage 28, 326–341. https://doi.org/10.1016/j.neuroimage.2005.05.032.

Ploner, M., Gross, J., Timmermann, L., Pollok, B., Schnitzler, A., 2006. Pain suppresses spontaneous brain rhythms. Cereb. Cortex 16, 537–540. https://doi.org/10.1093/cercor/bhj001.

Schulte, L.H., May, A., 2016. The migraine generator revisited: continuous scanning of the migraine cycle over 30 days and three spontaneous attacks. Brain 139, 1987–1993. https://doi.org/10.1093/brain/aww097.

Schulte, L.H., May, A., 2017. Of generators, networks and migraine attacks. Curr. Opin. Neurol. 30, 241–245. https://doi.org/10.1097/WCO.0000000000000441.

Schulte, L.H., Jürgens, T.P., May, A., 2015. Photo-, osmo- and phonophobia in the premonitory phase of migraine: mistaking symptoms for triggers? J. Headache Pain 16, 14. https://doi.org/10.1186/s10194-015-0495-7.

Schulte, L.H., Sprenger, C., May, A., 2016. Physiological brainstem mechanisms of trigeminal nociception: an fMRI study at 3T. NeuroImage 124, 518–525. https://doi.org/10.1016/j.neuroimage.2015.09.023.

Schulte, L.H., Allers, A., May, A., 2017. Hypothalamus as a mediator of chronic migraine: evidence from high-resolution fMRI. Neurology. https://doi.org/10.1212/WNL.0000000000003963.

Schwedt, T.J., 2013. Multisensory integration in migraine. Curr. Opin. Neurol. 26, 248–253. https://doi.org/10.1097/WCO.0b013e328360edb1.

Stankewitz, A., May, A., 2011. Increased limbic and brainstem activity during migraine attacks following olfactory stimulation. Neurology 77, 476–482. https://doi.org/10.1212/WNL.0b013e318227e4a8.

Stankewitz, A., Voit, H.L., Bingel, U., Peschke, C., May, A., 2010. A new trigemino-nociceptive stimulation model for event-related fMRI. Cephalalgia 30, 475–485. https://doi.org/10.1111/j.1468-2982.2009.01968.x.

Taesler, P., Rose, M., 2016. Prestimulus theta oscillations and connectivity modulate pain perception. J. Neurosci. 36, 5026–5033. https://doi.org/10.1523/JNEUROSCI.3325-15.2016.

Thomson, D.J., 1982. Spectrum estimation and harmonic analysis. Proc. IEEE 70, 1055–1096. https://doi.org/10.1109/PROC.1982.12433.

Tibber, M.S., Guedes, A., Shepherd, A.J., 2006. Orientation discrimination and contrast detection thresholds in migraine for cardinal and oblique angles. Invest. Ophthalmol. Vis. Sci. 47, 5599–5604. https://doi.org/10.1167/iovs.06-0640.

Vingen, J.V., Pareja, J.A., Støren, O., White, L.R., Stovner, L.J., 1998. Phonophobia in migraine. Cephalalgia 18, 243–249. https://doi.org/10.1111/j.1468-2982.1998.1805243.x.

Weiller, C., May, A., Limmroth, V., Jüptner, M., Kaube, H., Schayck, R.V., Coenen, H.H., Diener, H.C., 1995. Brain stem activation in spontaneous human migraine attacks. Nat. Med. 1, 658–660.

Westfall, P., Young, S., 1993. Resampling-Based Multiple Testing: Examples and Methods for p-Value Adjustment (Wiley Series in Probability and Statistics). Wiley-Interscience.